

SECOND EUROPEAN ROTORCRAFT AND POWERED LIFT AIRCRAFT FORUM

Paper No. 35

RECENT EXPERIENCE IN THE TESTING OF A GENERALIZED ROTOR
AEROELASTIC MODEL AT LANGLEY RESEARCH CENTER

C. E. Hammond and W. H. Weller

Langley Directorate
U.S. Army Air Mobility R&D Laboratory
NASA Langley Research Center
Hampton, Virginia 23665
U.S.A.

September 20 - 22, 1976

Bückeburg, Federal Republic of Germany

Deutsche Gesellschaft für Luft- und Raumfahrt E.V.

Postfach 510645, D-5000 Köln, Germany

RECENT EXPERIENCE IN THE TESTING OF A GENERALIZED ROTOR
AEROELASTIC MODEL AT LANGLEY RESEARCH CENTER

C. E. Hammond and W. H. Weller

Langley Directorate
U.S. Army Air Mobility R&D Laboratory
NASA Langley Research Center
Hampton, Virginia 23665
U.S.A.

1. ABSTRACT

The use of aeroelastically scaled helicopter rotor wind-tunnel models in establishing or verifying the dynamic characteristics of new or existing rotor designs is discussed. A model, termed the generalized rotor aeroelastic model (GRAM), which has been developed for testing aeroelastically scaled rotor models is described, and the utility of the model in being able to test a variety of rotor systems to meet a broad range of test objectives is demonstrated through presentation of data from recent tests. Data are presented from tests of an AH-1G Cobra model to determine whether or not the two-blade teetering rotor can experience stall flutter, tests of two wide chord teetering rotors to evaluate the effect of the wide chord on blade loads and rotor performance, and tests of a new four-blade flex-hinge rotor configuration to provide information for the designer relative to its dynamic characteristics. Recent tests of a variable geometry rotor are also described although final data are currently unavailable. Since the GRAM was developed for testing in a wind tunnel which has the capability of using Freon-12 as a test medium, some of the advantages of Freon-12 for testing of aeroelastically scaled models are also discussed.

2. INTRODUCTION

The use of aeroelastically scaled wind-tunnel models to establish the flutter boundaries for fixed-wing flight vehicles has been an established practice for many years. Garrick,¹ for example, states that the first aeroelastic investigation by means of a model of an aircraft prototype is believed to have been in 1938. It was not until the mid-1950's, however, that the testing of an aeroelastically scaled model became a routine part of the development cycle of new fixed-wing aircraft. Today, these models are tested not only to provide data for confirmation of the analytical results but in flight regimes where adequate analytical tools are nonexistent, such as the transonic regime, they provide the only source of information relative to the flutter boundary prior to actual flight test of the vehicle.

In the past, the helicopter industry has not relied as heavily on wind-tunnel testing of aeroelastically scaled models as has their fixed-wing counterparts. The primary reason for this has been that each new

helicopter rotor represented only a slight extrapolation from previous rotor designs. Also, helicopter designers were willing to accept the weight penalties associated with ultra-conservative aeroelastic designs for rotor blades since autorotation requirements generally dictate the amount of mass required in the rotor. These design practices resulted in rotor blade designs for which the aeroelastic behavior was reasonably well understood and generally aeroelastic model tests were not deemed necessary.

Recently, however, the advent of new rotor systems with unique dynamic characteristics, such as the hingeless rotor, has resulted in increased emphasis being placed on wind-tunnel testing of aeroelastically scaled helicopter rotor models. Miao et al.² have described the significant impact which aeroelastic model tests had on the development of the Boeing Vertol entry in the U.S. Army UTTAS competition. It is to be expected that if the helicopter is to continue in its development, then the design philosophy of build it, fly it, fix it, which has until recent years prevailed in the helicopter industry, must be supplanted by a systematic series of analyses, model tests, and flight tests with each step of the process being guided by all of the previous steps.

In anticipation of future needs, the Langley Directorate, USAAMRDL, and NASA Langley Research Center have developed the capability for testing aeroelastically scaled models of current and advanced helicopter rotor configurations. The model is termed the generalized rotor aeroelastic model (GRAM), and it was developed primarily to support Army and NASA research in the general area of rotorcraft aeroelasticity. The model is to be used to generate data for correlation of analytical tools, to support in-house flight research vehicles such as the Rotor Systems Research Aircraft under development by the Army and NASA, and to support cooperative research programs between the government and industry. This paper will describe the GRAM and the manner in which it is used. Several recent tests will be discussed to illustrate the versatility of the model in being able to test a variety of rotor systems to meet a broad range of test objectives. Significant data will be presented to show the utility of the model in verifying the aeroelastic characteristics of helicopter rotor configurations. Some advantages of Freon-12 as a wind-tunnel test medium are also discussed.

3. SYMBOLS

a	Airfoil lift curve slope
c	Blade chord
\bar{c}	Speed of sound
C_D	Rotor drag coefficient
C_L	Rotor lift coefficient
C_T	Rotor thrust coefficient
C_Q	Rotor torque coefficient
g	Gravitational constant

I_f	Blade flapping mass moment of inertia
M_T	Blade tip Mach number at 90° azimuth
P	Pressure
R	Rotor radius
\bar{R}	Gas constant
T	Temperature
V	Linear velocity
α_s	Rotor shaft angle
γ	Ratio of specific heats
ΔA_i	Longitudinal cyclic change from trim-to-shaft condition
θ_c	Blade collective pitch at 3/4 radius
μ	Coefficient of viscosity
ρ	Test medium density
σ	Rotor solidity, ratio of blade area to total disk area
ω	Structural frequency
Ω	Rotor rotational speed

4. THE GENERALIZED ROTOR AEROELASTIC MODEL

The generalized rotor aeroelastic model (GRAM) is shown in Figure 1 with a four-bladed rotor and installed in the transonic dynamics tunnel at the NASA Langley Research Center. The model is configured for testing model rotors with diameters ranging from 2.74 to 3.35 meters (9 to 11 ft). Some of the more important structural features of the model are shown in Figure 2. The frame of the model, which is normally enclosed by a fiberglass and aluminum shell, is attached by four elastomeric mounts to an internal base plate such that the model has some freedom of motion in pitch, roll, and vertical translation. By proper selection of the mount stiffness, full-scale rigid body or suspension system frequencies, which are especially important in testing of two-bladed teetering rotors,³ can be simulated.

The GRAM is powered by two variable frequency, water-cooled synchronous electric motors. Each motor is rated at 47 horsepower at a speed of 12000 rpm. The motors are connected to the rotor shaft through a two-stage speed reduction system which provides a maximum rotor speed of 1540 rpm. Rotor speed is controlled by varying the line frequency to the electric motors.

The model also features a complete set of helicopter controls. The floating swashplate is raised or lowered to achieve collective pitch inputs and tilted longitudinally or laterally to provide cyclic pitch motions of the blades. The swashplate motions are controlled by three electrohydraulic servo-actuator assemblies which provide not only the mean control settings required for a given rotor trim condition, but also allow for oscillatory inputs about the mean. The oscillatory inputs, which may be at frequencies up to approximately 50 Hz, are useful in determining rotor frequency response and in performing subcritical aeroelastic stability testing wherein frequency and damping information is obtained for critical modes as a stability boundary is approached. Available oscillatory inputs include forward and regressive stick sticks; pitch, roll, and collective doublets; and an input having a constant power spectral density (PSD). With the exception of the constant PSD input, these excitations are identical to the types of inputs required by the U.S. Army in full-scale flight testing of helicopters.

In order to simulate helicopter forward flight trim attitudes, the pitch attitude of the base plate inside the model can be remotely changed by electromechanical actuators. Model attitudes from 20° nose down to 8° nose up may be obtained.

The GRAM is instrumented to read out all model control settings including model angle of attack, collective pitch, longitudinal and lateral cyclic pitch and rotor speed. All three components of body translational acceleration are measured by accelerometers mounted as near to the fuselage center of gravity as practical. The rotating blade data are transferred to the fixed system using a 60-ring, horizontal disk slip ring assembly which can accommodate up to 26 channels of rotating system data. The combined rotor and fuselage forces and moments are measured using a six-component strain-gage balance mounted below the base plate.

The model is "flown" using control switches and displays located on the model operator's console. Switches controlling model pitch attitude, collective pitch, and longitudinal and lateral cyclic pitch are mounted on the console face. Displays of these control settings as well as displays of blade first harmonic flapping coefficients and selected rotor loads are presented in engineering units on digital panel meters. Rotor and drive motor speeds are given on a digital frequency counter. The motor speeds are selected from a second console which contains controls for the variable frequency motor-generator set. Various warning lights and alarms are also installed on the model operator's console to indicate approach to critical operating conditions.

5. TEST FACILITY AND MODEL SCALING

Aeroelastic rotor testing is presently conducted at the Langley transonic dynamics tunnel (TDT) shown in Figure 3. The TDT is a continuous-flow tunnel which is capable of operation over a Mach number range from 0 to 1.2 at pressures ranging from 1376 N/m² (0.2 psia) to full atmospheric pressure. The tunnel test section is 4.9 meters (16 ft) square with a cross-sectional area of 23 m² (248 ft²). One of the unique features of this facility is the capability for testing in either air or Freon-12 test mediums. Suitability of Freon-12 as a wind-tunnel test medium is discussed in References 4 and 5. Freon-12 is a gas which is heavier than air by a factor of

approximately 4 and has a speed of sound below one-half that of air for corresponding temperatures and pressures. Use of Freon-12 offers several advantages for model rotor testing as will be discussed in a subsequent section.

5.1 Data Acquisition

The TDT has recently been equipped with a computer controlled data acquisition system. This system, shown in Figure 4, consists of a Xerox Sigma-5 digital computer coupled to 60 analog data channels. The analog data from the transducers on the model are converted to digital form for computer processing by an analog-to-digital converter which can sample the data stream at up to 50000 samples per second. The data may be recorded in either analog or digital form. For analog recording, 12 channels may be recorded directly on the intermediate-band analog recorder or up to 60 channels may be frequency multiplexed onto the low-band multiplex tape recorder. Generally, during a wind-tunnel test, the analog mode is the primary means for recording data, with only those data which are to be analyzed on-line being digitized. All of the analog front-end equipment may be operated either manually or under computer control. This permits one to configure the analog front-end dynamically during a given run to obtain the best possible data.

The digital computer also allows one to reduce data on-line and to perform various analyses of the data. This capability permits the test engineer to better select upcoming test points and to determine the quality of the data from previous test points. The interactive computer graphics capability provided by the graphics display unit in the tunnel control room is having a significant impact on the manner in which tunnel tests are conducted⁶ and it is expected that as software development for the data system continues, this piece of equipment will foster the development of new and more efficient techniques for conducting aeroelastic model tests. This capability is currently being utilized in the GRAM tests to monitor the aeroelastic stability characteristics of the rotor blades as a function of the test conditions.

5.2 Aeroelastic Model Scaling

In aeroelastic model studies, the model must not only be geometrically similar to the full-scale vehicle, but the model stiffness, mass, and inertial properties must simulate those of the full-scale structure. Further, the ratio of structural density to test medium density must be the same for model and full scale. Table 1 presents some of the more important parameters considered in the design of an aeroelastically scaled rotor model. Typical scale factors are presented for air and Freon-12 test mediums and a 1/5-scale model.

Ideally, the Mach number, Reynolds number, and Froude number should be the same for the model and full scale. However, when operating a reduced size model in air at or below atmospheric pressure, it is impossible to match more than one of these parameters due to conflicting design or operating requirements. Reynolds number similarity is generally sacrificed in aeroelastic model testing since its influence on the aeroelastic stability

boundaries of the model is usually secondary to the effects of Mach number and Froude number. Therefore, aeroelastic models are generally referred to as being Mach-scaled or Froude-scaled.

If compressibility effects are important to the aeroelastic phenomena being investigated, then the Mach number is matched between the model and full scale. If the gravity forces are significant as compared to other forces acting on the model, and if compressibility effects may be considered secondary, then the Froude number of the model is matched to that of the full-scale vehicle. In the case where both Mach number and Froude number are important, the designer is faced with a dilemma. The use of Freon-12 provides a solution to this situation. If a 1/5-scale model is used, then Mach number and Froude number similarity may be satisfied simultaneously.

Some other important consequences of the use of Freon-12 are also indicated in Table 1. For example, the rotor speed required for a given tip Mach number in Freon-12 is approximately one-half that required in air. Further, the power required in Freon is much less than that required in air. This not only means that the power required for the model is less but also the power required to operate the tunnel is less with Freon than with air, thus making the tunnel more efficient from an energy standpoint. The Reynolds number is also much higher in Freon-12 than in air. Reynolds number has a strong influence on the maximum aerodynamic forces generated by an airfoil, and thus the higher Reynolds number capability of Freon-12 is a strong asset to the measurement of rotor performance and blade loads, particularly when stalling is expected over portions of the blades. Finally, since Freon-12 is four times as dense as air, the model scaled for Freon-12 may be heavier, and thus less expensive, than its air-scaled counterpart.

6. ROTORS TESTED ON THE GRAM

The rotors which have been tested to date on the GRAM are shown pictorially in Figure 5. These rotors include an AH-1G Cobra rotor, a new four-bladed flex-hinge rotor being developed by Bell Helicopter Textron, a teetering rotor system in which the blade chord was increased substantially over that of currently operational teetering rotors, and a model of the variable geometry rotor. In all the rotor tests which are conducted using the GRAM, both rotor performance and blade dynamic response data are measured so that the overall operational characteristics of the rotors may be determined.

6.1 Conventional Cobra Rotor

The Cobra rotor was a 1/4-size rotor which was dynamically similar to a full-scale AH-1G rotor and Mach-scaled for operation in Freon-12 at atmospheric pressure in order to best approximate the Mach number and Reynolds number characteristics of the full-scale rotor. The model had a diameter of 3.35 m (11 ft) and a blade chord of 17.15 cm (6.75 in.). The primary purpose of the test was to determine whether or not two-bladed teetering rotors experience the stall flutter phenomenon which, for several years, has been one of the primary factors limiting the forward flight speeds of articulated rotors. This phenomenon is characterized by high oscillatory blade loads at the first torsional frequency of the blade occurring as the blade traverses

the retreating side of the rotor disk. It has been speculated that because of the unique dynamic characteristics of the two-bladed teetering rotor this rotor type does not exhibit stall flutter characteristics.

Blade loads and rotor performance data were obtained on the Cobra model rotor at normal and high thrust conditions for advance ratios up to 0.40. In order to compare the model test conditions with the full-scale flight envelope, the model thrust values for selected test points were converted to full-scale load factors and plotted on the aircraft flight envelope as shown in Figure 6. From this figure it may be seen that model data corresponding to full-scale thrust values outside the sustained operating envelope of the aircraft, but within the maneuver envelope, were obtained. Numerous other data points within the sustained and maneuver envelopes were obtained, but in the interest of clarity, these points were not plotted on the figure. Note that the model tests do not simulate maneuvers, rather the thrust on the model simulates the full-scale thrust required in maneuvering flight.

For the test points on the figure, the model blade torsional moment waveforms at 45% radius are shown for two rotor revolutions. Note that for the low advance ratio and low thrust condition the torsional waveform does not indicate any oscillations on the retreating side of the disk. However, for the low advance ratio high thrust condition and for the high advance maneuver thrust condition, there are significant torsional oscillations of the model blade on the retreating side of the disk. These oscillations are at the first torsional frequency of the rotor. It should be noted that, although the rotor model was scaled, the torsional frequency was approximately a factor of 2 higher than scale due to the stiff GRAM control system. The occurrence of stall flutter during these tests suggests that no characteristic unique to two-bladed teetering rotors is responsible for the seeming nonexistence of this problem in flight hardware. The fact that production teetering rotors have torsional frequencies approximately one-half those associated with most articulated rotors is thus the most likely explanation of why stall flutter is not significantly manifested in currently operational teetering rotors.

6.2 Wide Chord Teetering Rotor

The wide-chord teetering rotor shown in Figure 5 was approximately 1/6-scale with a diameter of 3.26 m (10.7 ft) and a blade chord of 25.4 cm (10 in.). Two wide-chord rotors were tested; one had midspan flapping hinges as shown in Figure 5 while the other had no midspan hinges. Except for the midspan hinges, the rotors were aeroelastically matched and both were Mach-scaled for operation in Freon-12 at atmospheric pressure. The purpose of the test was to evaluate the use of a wider chord for increasing the lift capabilities of the two-bladed teetering rotor and to obtain data on the level of the resulting blade loads. A further purpose of the test was to determine the effectiveness of a midspan flapping hinge in reducing the beamwise blade loads. This last objective dictated that two rotors must be tested, one with the hinge and one without the hinge. The question of whether or not the rotor with the hinges would exhibit any unusual dynamic characteristics was also of concern before the test.

Figure 7 shows a comparison of the oscillatory blade loads in the beamwise direction as a function of spanwise position for the rotors with and without the midspan hinge. As may be seen from the figure, the hinge was quite effective in reducing the oscillatory beamwise bending moments over a large portion of the span. The inplane moments were not decreased by addition of the flapping hinge. The hinged rotor exhibited no tendency to become dynamically unstable, nor were the outboard blade motions excessive. From an operational point of view, the hinged blades behaved quite similarly to the rotor without the hinge.

6.3 Four-Bladed Flex-Hinge Rotor

The four-bladed flex-hinge rotor shown in Figure 5 was a 1/5-scale model with a diameter of 3.05 m (10 ft) and a chord of 10.77 cm (4.24 in.). The rotor is hingeless in the flapping direction, employing flexures having low bending stiffness to accommodate the flapping motions of the blades. In the lead-lag direction the blades are hinged, but an elastomeric damper is employed which not only provides inplane damping, but also contributes significantly to the inplane stiffness, causing the rotor to behave dynamically as a soft-inplane hingeless rotor. The model was Froude-scaled for operation in air since a major portion of the program involved blade motion stability tests in hover which were conducted at another test site.

The objectives of the tests were to provide performance and loads characteristics of the rotor and to evaluate the aeroelastic stability characteristics with various levels of blade lead-lag damping and several configurations of kinematic coupling between the different blade degrees of freedom. The model tests were to guide the development and eventual flight test of the full-scale hardware by Bell Helicopter Textron as a part of its in-house research and development program. Two wind-tunnel entries with the model rotor provided a voluminous amount of data on both the dynamics and performance characteristics of this new rotor design.

Figure 8 presents a typical sample of the rotor performance data which were obtained for the flex-hinge rotor at an advance ratio of 0.35. Shown on the figure are plots of model power coefficient versus thrust coefficient and model lift coefficient versus drag coefficient for three values of model shaft angle of attack. This type of information is obtained over the complete operational spectrum for all rotors tested on the GRAM and it is useful to the designer in determining how a given helicopter design employing the test rotor could be expected to perform. For example, from the power versus thrust plot, the designer can determine the power required for various flight conditions and thus arrive at the installed power required for the aircraft.

It is common practice in wind-tunnel testing of model rotors to obtain the data with the rotor flapping trimmed to zero with respect to the shaft, and the performance data in Figure 8 were obtained in just this manner. In order to evaluate the effect of trim conditions on blade loads, data were obtained from the flex-hinge rotor for varying amounts of longitudinal cyclic pitch or blade flapping at a constant lift coefficient. The hub beamwise and chordwise bending moments at an inboard station on the blade for an advance ratio of 0.30 are shown in Figure 9. From the figure it may be seen that, as might be expected, the longitudinal flapping of the rotor has

a significant influence on the beamwise moments, but a lesser influence on the chordwise moments. Based on these data, it is felt that if a purpose of the model test is to supply blade loads data for the designer or to correlate the model blade loads data with flight-test data or analysis, then the model data must be obtained at realistic trim conditions. It is also felt that some of the lack of correlation in the past between analyses, model tests, and flight tests may be due to the fact that the trim conditions were not the same for all the data being correlated.

One of the concerns at the outset of the flex-hinge model program was that the phenomenon of air resonance. In order to be able to examine the susceptibility of the flex-hinge rotor to this condition, a subcritical testing technique was developed wherein the frequency and damping in the mode of interest can be determined on-line at each test condition⁶ and, by monitoring the damping as a function of the test parameters, indications of approach to a stability boundary may be observed.

The subcritical damping technique, known as the moving-block technique,⁷ was implemented interactively on the TDT data acquisition system for use on-line during the flex-hinge rotor tests. Figure 10, which is a reproduction of the information presented to the engineer on the graphics display unit for one of the flex-hinge data points, may be used to illustrate the technique. The lower-left quadrant of the figure is the lead-lag response of one of the blades to a forward stick stir of the GRAM control system. The total Fourier transform of the response is plotted in the upper-left quadrant and the engineer may selectively display a portion of the total transform in the lower-right quadrant. From either of these plots of the response frequency spectrum, the engineer selects the frequency of the mode to be analyzed by identifying the peak in the spectrum corresponding to the mode of interest. The time decay of this peak is determined by computing the amplitude of the peak for successive time segments of the response record. By plotting the variation in time of the logarithm of the peak amplitude, the plot in the upper-right quadrant of Figure 10 is obtained. The slope of a least-squares linear fit to the initial sloping portion of this plot is proportional to the damping in the mode being analyzed. The oscillations which occur in this plot at later times stem from the presence of other modes, as well as noise, in the response data. The computed frequency and damping for the selected mode are presented in the lower portion of the display.

Although no instabilities were experienced on the flex-hinge rotor, damping trends were obtained for various levels of inplane damping to determine an optimum level of damping from both a stability point of view and a blade response standpoint. Figure 11 shows the trend of damping for the blade lead-lag mode as a function of advance ratio for the nominal dmaper configuration. As may be seen, the mode is quite highly damped and no tendency toward instability is indicated. A more detailed discussion of the flex-hinge tests may be found in Reference 8.

6.4 Variable Geometry Rotor

Tests of the variable geometry rotor (VGR) shown in Figure 5 have just recently been concluded. The VGR is essentially two three-bladed rotor systems stacked one on top of the other with the vertical separation and azimuthal indexing between the two rotor systems being variable. The model

was a 1/7-scale fully articulated configuration with a diameter of 2.74 m (9 ft) and a blade chord of 6.83 cm (2.69 in.). It was Mach-scaled in air since it was anticipated that the model would be tested in other wind-tunnel facilities. The objectives of the test program were to identify the optimum combination of rotor spacings from a performance standpoint and to determine if such a configuration was susceptible to excessive blade loads and adverse handling characteristics during forward flight as a result of the aerodynamic interference between the two rotor systems. Data resulting from the test are not currently available.

7. CONCLUDING REMARKS

This paper has dealt with the testing of aeroelastically scaled helicopter rotor models using the generalized rotor aeroelastic model (GRAM). The tests conducted to date have illustrated the utility of the GRAM in providing information relative to the dynamic characteristics of both existing rotor configurations and new rotor configurations being considered for full-scale hardware development programs. It is expected that if the evolutionary cycle of the helicopter follows the same path as that of the fixed-wing aircraft, then aeroelastic model tests will become an integral part of future helicopter development programs. Future test programs involving the GRAM include tests of research rotor configurations to provide data for correlation of analytical tools, tests of existing rotor designs to explore means for reducing helicopter fuselage vibration levels, tests of new rotor configurations proposed for flight test on the Rotor Systems Research Aircraft, and cooperative test programs with industry to provide test data on research configurations in order to advance the state of the art in rotor design.

8. ACKNOWLEDGMENTS

The authors gratefully acknowledge the assistance of Bell Helicopter Textron personnel in the design, manufacture, and testing of the flex-hinge and wide-chord rotors.

9. REFERENCES

1. I. E. Garrick, Some Concepts and Problem Areas in Aircraft Flutter. SMF Fund Paper No. FF-15, Inst. Aero. Sci., 1957.
2. W. L. Miao and H. B. Huber, Rotor Aeroelastic Stability Coupled With Helicopter Body Motion. Rotorcraft Dynamics, NASA SP-352, 1974, pp. 137-146.
3. J. A. White and C. D. Lee, Effect of Hub Impedance on the Oscillatory Blade Loads of a Two-Bladed Rotor System. Presented at the AHS 30th Annual National Forum, Washington, D.C., May 7-9, 1974. Preprint No. 832.
4. Albert E. von Doenhoff, Albert L. Braslow, and Milton A. Swartzberg, Studies of the Use of Freon-12 as a Wing Tunnel Testing Medium. NACA TN-3000, 1958.

5. D. M. Pozniak, Investigation Into the Use of Freon-12 as a Working Medium in a High Speed Wind Tunnel. College of Aeronautics, Cranfield (Great Britain), Note No. 72, November 1957.
6. R. V. Doggett, Jr., and C. E. Hammond, Application of Interactive Computer Graphics in Wind Tunnel Dynamic Model Testing. Applications of Computer Graphics in Engineering, NASA SP-390, 1975, pp. 325-353.
7. William D. Anderson, Investigation of Reactionless Mode Stability Characteristics of a Stiff Inplane Hingeless Rotor System. Preprint No. 734, Proceedings of the 29th Annual Forum of the American Helicopter Society, May 1973.
8. Bill White and William Weller, The Flexhinge Rotor. Presented at the American Helicopter Society Mideast Region Symposium on Rotor Technology, Essington, Pennsylvania, August 1976.

TABLE 1. TYPICAL AEROELASTIC SCALING PARAMETERS FOR A ONE-FIFTH-SCALE MODEL IN AIR AND FREON-12 TEST MEDIUMS*

Parameter	General scaling formula	Scale factors**	
		Air	Freon-12
Speed of sound (\bar{c})	$\sqrt{\gamma \bar{R} T}$	1	0.448
Density (ρ)	$P/\bar{R}T$	1	4.0
Coef. of viscosity (μ)	—	1	.705
Length (R)	R	.2	.2
Mass	$R^3 \rho$.008	.032
Angular velocity (Ω)	\bar{c}/R	5	2.24
Power	$R^2 \rho \bar{c}^{-3}$.04	.0143
Mach number	V/\bar{c}	1	1
Froude number	\bar{c}^2/gR	5	1
Reynolds number	$\rho VR/\mu$.2	.508
Advance ratio	$V/\Omega R$	1	1
Locke number	$\rho a c R^4 / I_f$	1	1
Structural frequencies	ω/Ω	1	1

* Based on full atmospheric pressure and standard day conditions.
 ** Scale factor equals ratio of model to full-scale values.

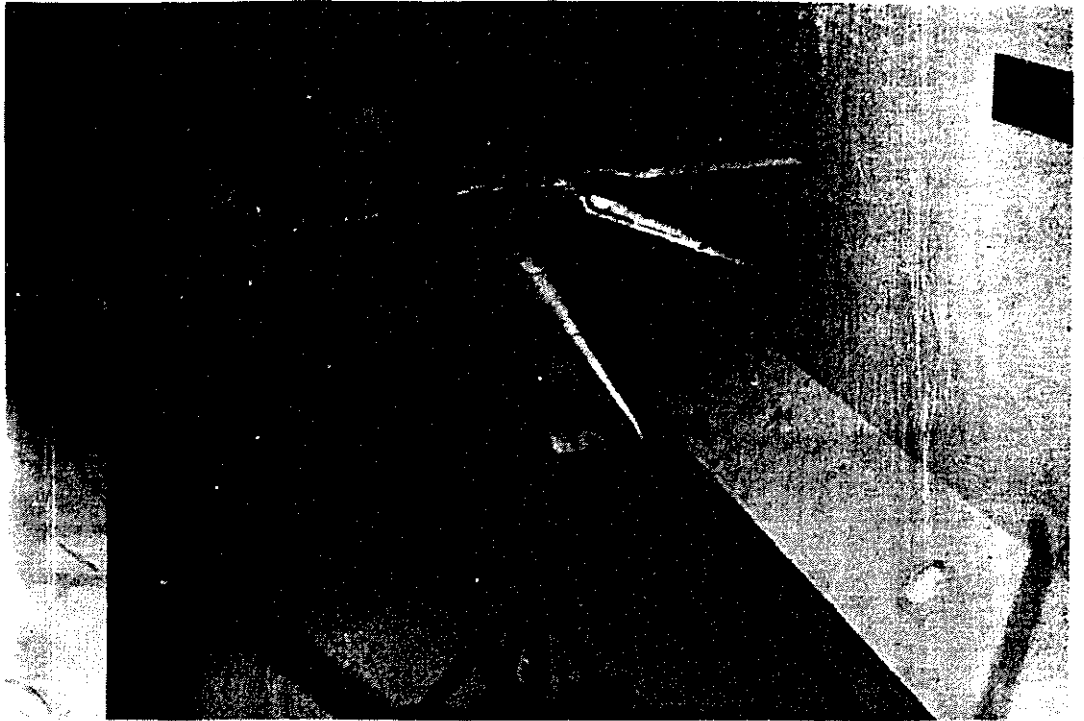


Figure 1. Generalized rotor aeroelastic model (GRAM) installed in the NASA Langley transonic dynamics tunnel.

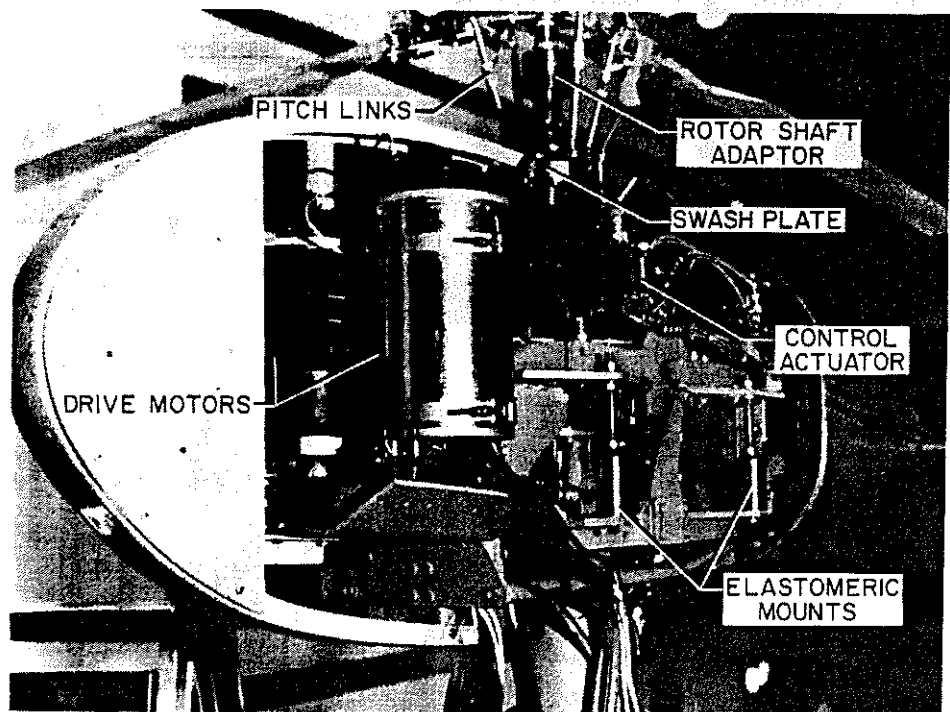


Figure 2. Detail of generalized rotor aeroelastic model.

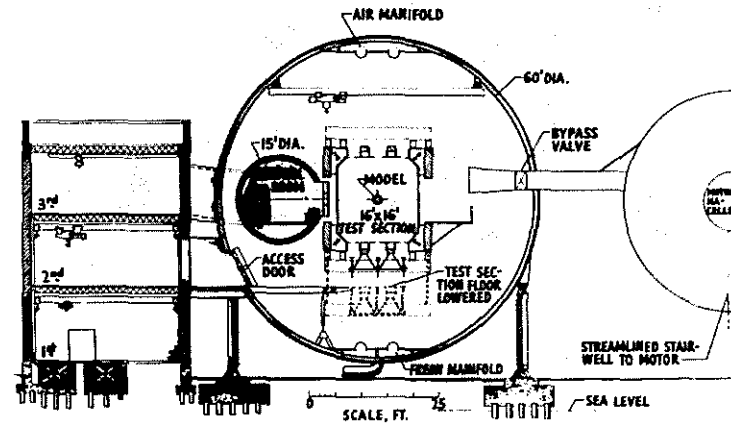
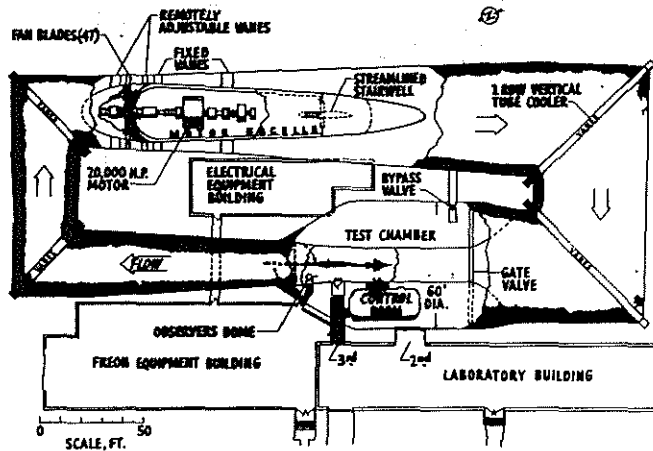
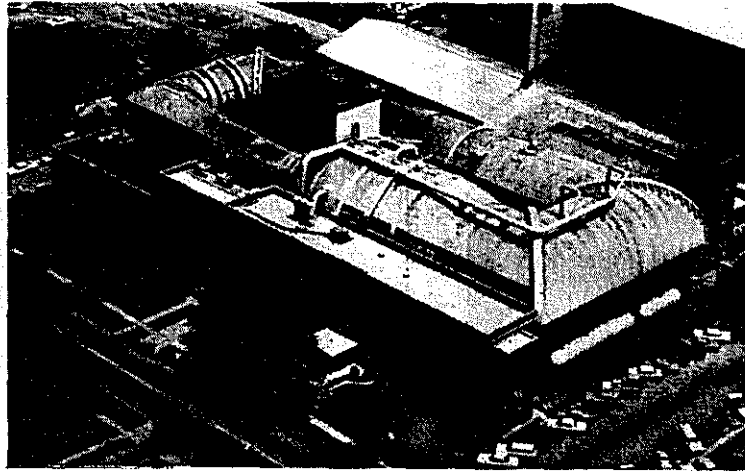


Figure 3. NASA Langley transonic dynamics tunnel.

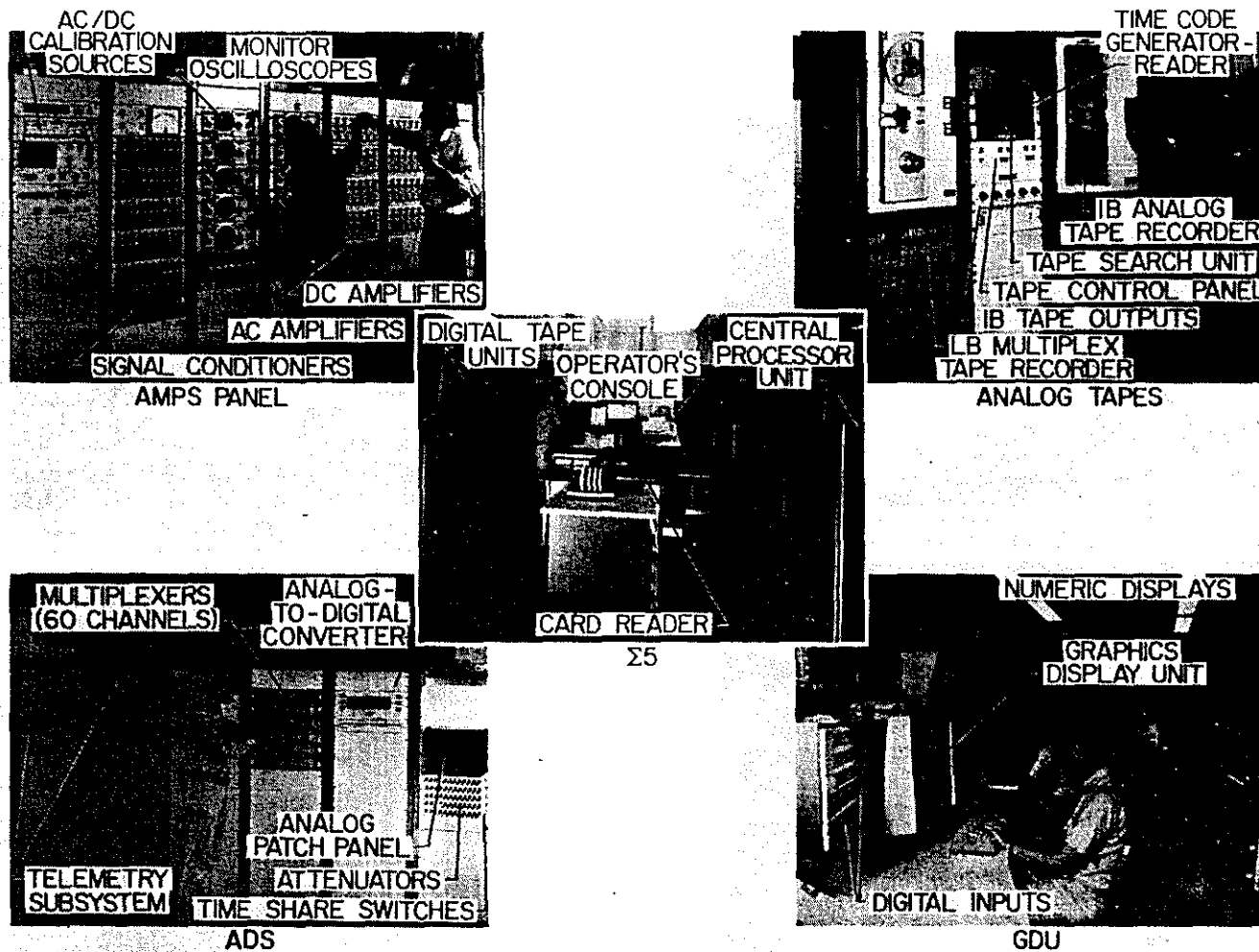
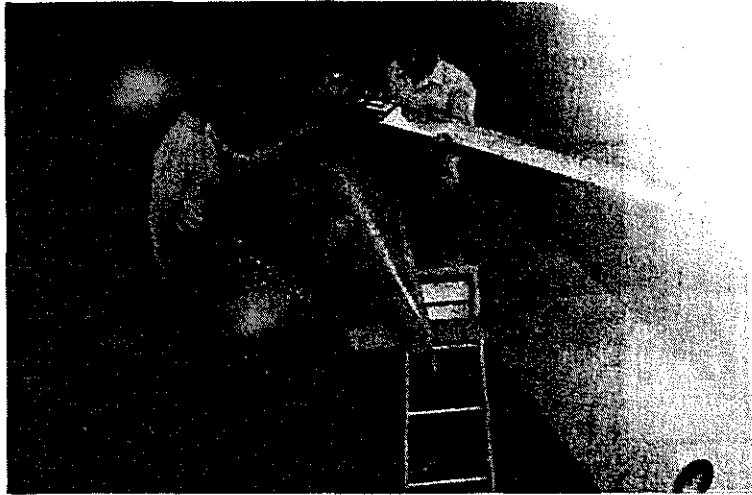


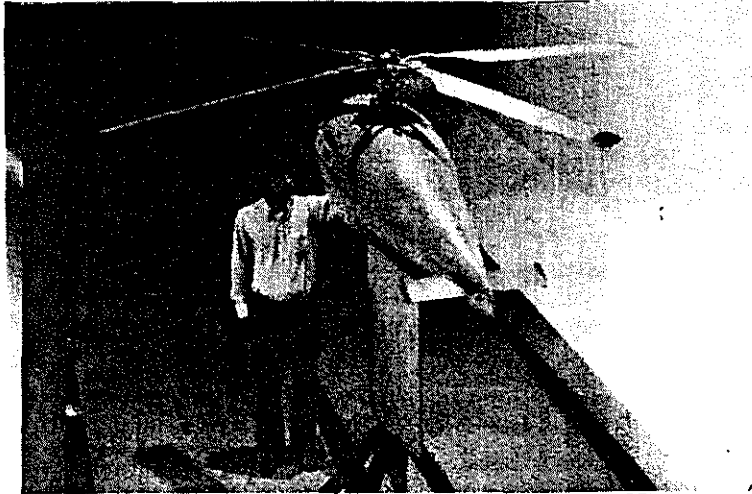
Figure 4. Transonic dynamics tunnel data acquisition system.



AH-IG COBRA ROTOR



WIDE CHORD ROTOR WITH HINGE



BELL FLEX-HINGE ROTOR



VARIABLE GEOMETRY ROTOR

Figure 5. Rotors which have been tested on the GRAM.

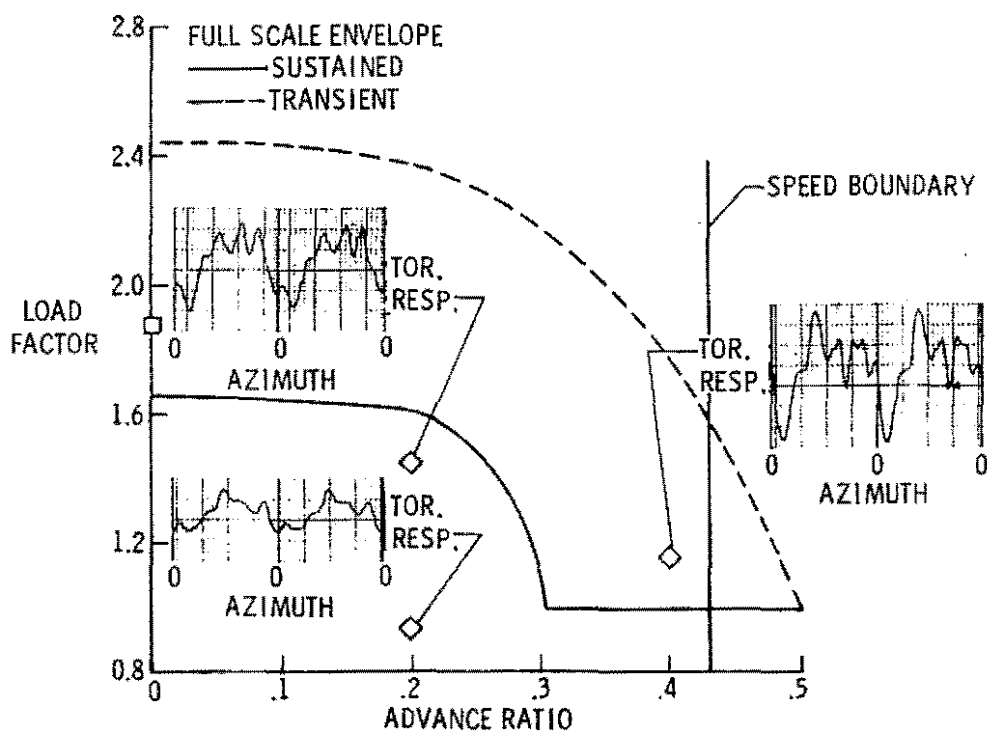


Figure 6. Model Cobra test conditions compared to full-scale flight envelope with selected blade torsional waveforms.

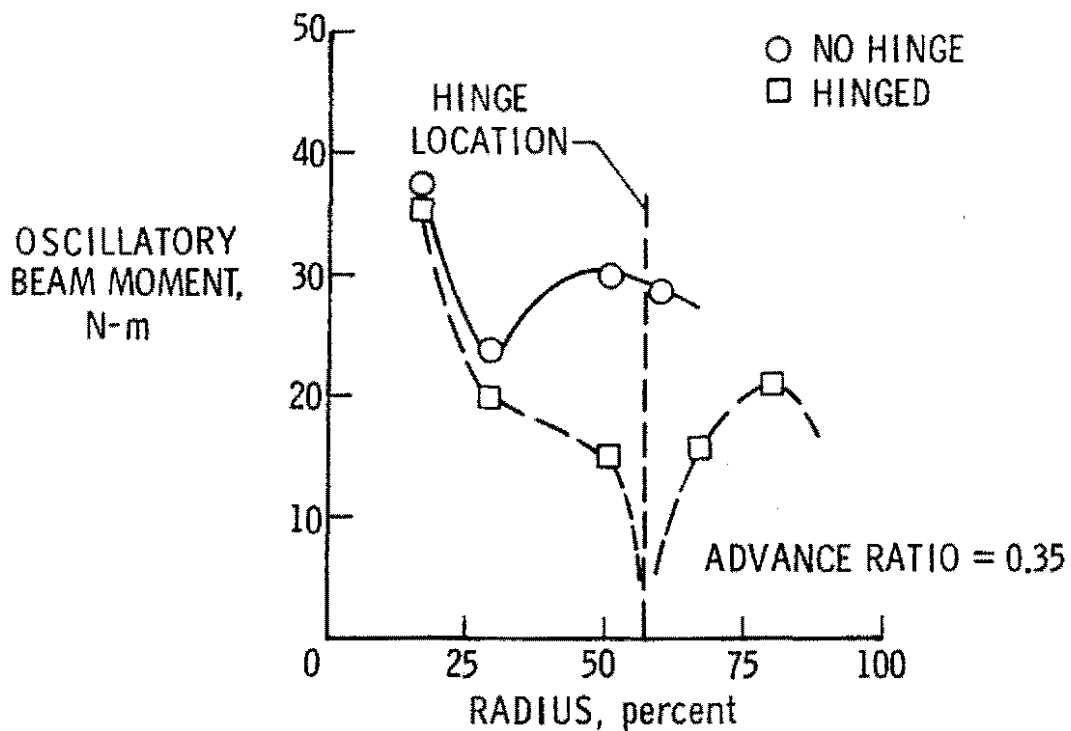


Figure 7. Comparison of oscillatory blade loadings as a function of span for the wide-chord teetering rotors.

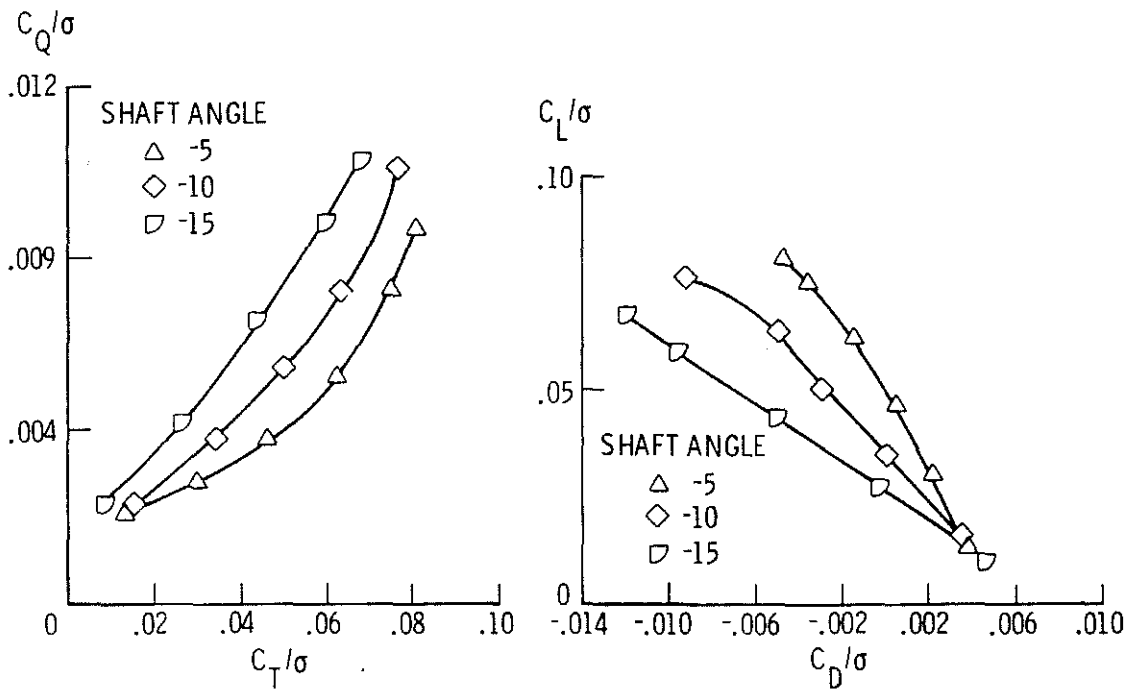


Figure 8. Rotor performance data for the flex-hinge rotor at an advance ratio of 0.35.

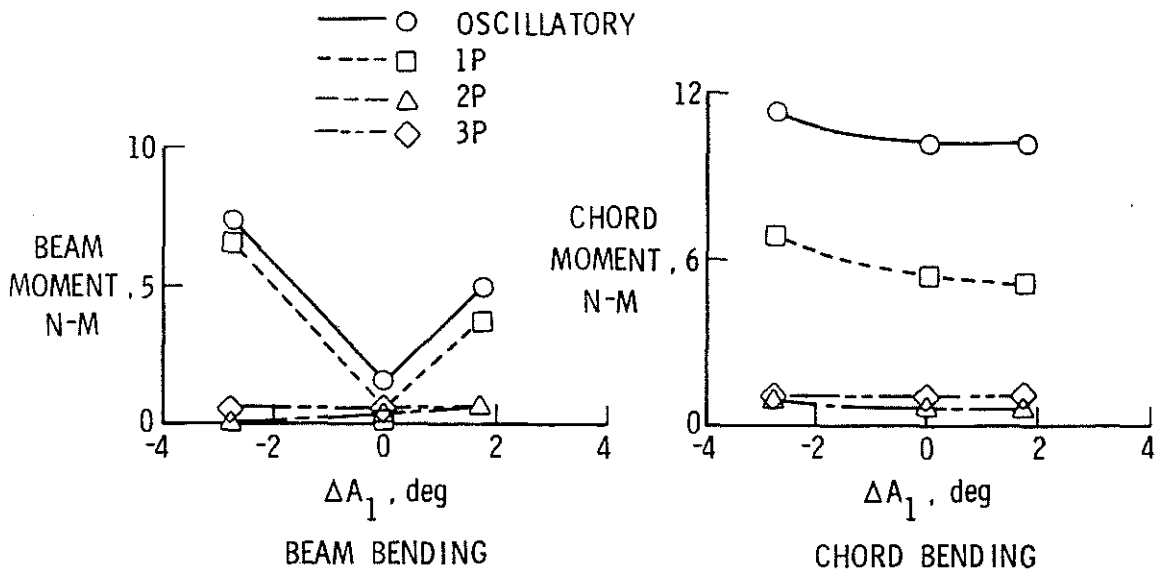


Figure 9. Variation of flex-hinge hub bending moments with trim state. Advance ratio = 0.3, $\alpha_s = -6.6^\circ$, $C_L/\sigma = 0.06$.

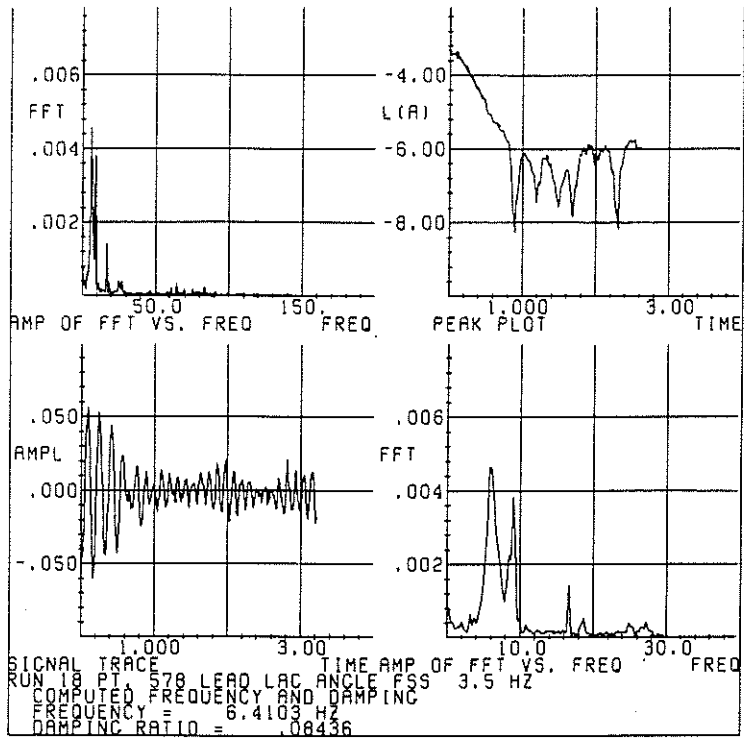


Figure 10. Typical moving-block results from flex-hinge model tests.

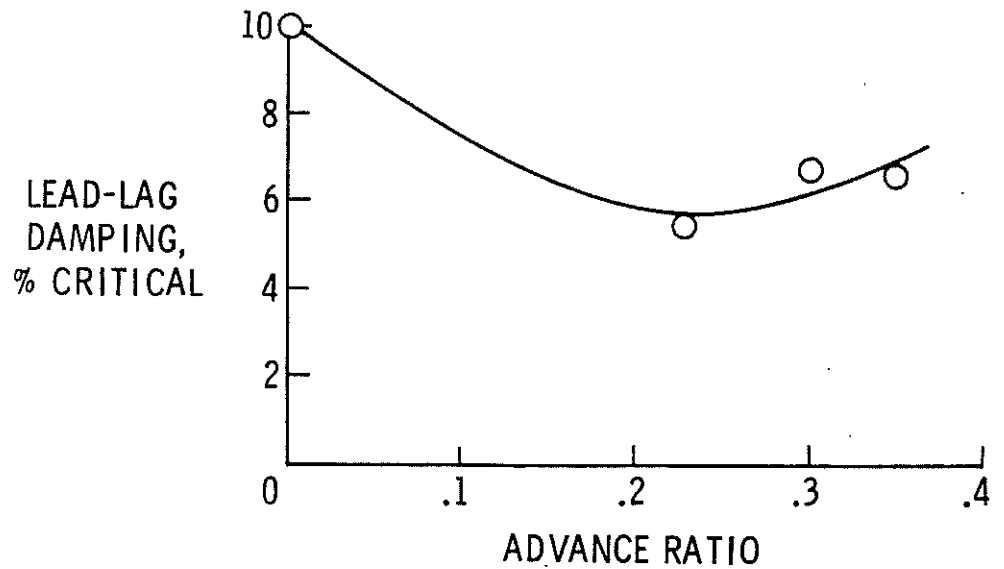


Figure 11. Blade lead-lag mode damping as a function of advance ratio for the model flex-hinge rotor.